

An Efficient Calibration Method for Triaxial Gyroscope

Li Wang, Steven Su, *Senior Member, IEEE*,

Abstract—This paper presents an efficient servomotor-aided calibration method for the triaxial gyroscope. The entire calibration process only takes about one minute, and high-precision equipment is not used. The main idea of this method is that the measurement of the gyroscope should equal to the rotation speed of the servomotor. A six-observation experimental design is proposed to minimize the maximum variance of the estimated scale factors and biases. Besides, a fast converged recursive linear least square estimation method is presented to reduce computational complexity. The simulation results specify the robustness under normal and extreme condition. We experimentally demonstrate the achievability of the proposed method on a robot arm and implements the method on a microcontroller. The calibration results of the proposed method are verified by comparing with a traditional turntable method, and the experiment indicates that the error between these two methods is less than 10^{-3} . By comparing the calibrated low-cost gyroscope reading with the reading from a high-precision gyroscope, we can infer that our method significantly increases the accuracy of the low-cost gyroscopes.

Index Terms—gyroscopes, angular velocity, calibration, experimental design, parameter estimation.

I. INTRODUCTION

Micro-electro-mechanical-system (MEMS) triaxial gyroscopes are widely used device for measuring angular velocity in many application, such as indoor pedestrian positioning [1], health monitoring [2], and consumer electronic devices [3], [4]. The precision of such low-cost gyroscope usually is not high, and the drift error will accumulate due to the integration when calculating the attitude [5]. Besides, the low repeatability and instability of the gyroscope cause the scale factor and biases change on every boot or under different environmental conditions, such as temperature change [6]. Therefore, the gyroscope needs to be calibrated before each use or when the environmental conditions change. Frequent calibration requires simple and efficient calibration methods.

The issue of gyroscope calibration has received considerable critical attention. The ordinary triaxial gyroscope calibration method requires rotating the gyroscope at known angular velocity [7]. This method can achieve high calibration accuracy while the complex calibration procedure and expensive calibration equipment make it unsuitable for use outside the laboratory. Gyroscope calibration methods that do not require precise rotation velocity measurements are presented in [8], [9], [10],

[11]. In [8], a camera is employed to provide the position and orientation information for gyroscope calibration. This method requires first to align the body frame and the image frame and calibrate the camera to achieve high accuracy. As the image is involved, the computational complexity is significantly increased. In [9], a magnetometer-aided calibration method is proposed. The gyroscope calibration reference is provided by an artificial homogeneous magnetic field. Obviously, it is not easy to build such a magnetic field outside the laboratory. In [10], [11], accelerometer-aided gyroscope calibration methods are proposed. The accelerometer is first calibrated by gravity using the multi-position method. Then, the accelerometer will provide the rotation speed of the gyroscope. The entire calibration takes more than 10 minutes. Besides, the error caused by the accelerometer may also be superimposed on the gyroscope parameters. However, it is important to find a fast and simple in-field calibration method for gyroscopes. This paper proposed a servomotor-aided gyroscope calibration method, which does not require high precision equipment and easy to implement outside the laboratory.

To meet the requirements of frequent calibration, improving calibration efficiency deserves a careful study. Most previous studies [7], [8], [9], [10], [11], [12] did not pay enough attention to investigating the selection of optimal experiments scheme. Until recently, a six-position accelerometer calibration experimental design (DoE) was proposed in [13]. The purpose of DoE is to obtain enough information to calibrate the accelerometer with a minimum of experiments. However, to the best of our knowledge, such DoE has not been applied to gyroscope calibration yet. In this study, a G-optimal DoE is proposed for gyroscope calibration, minimizing the maximum estimation variance over the entire measurement range.

For solving the regression problem, [14], [11], [15] applied nonlinear estimation methods, such as Nelder–Mead method [16] and Levenberg–Marquardt algorithm [17]. These methods always need large computational power. However, a gyroscope is often a part of an embedded system with limited resource and battery life. Therefore, we proposed a fast converged recursive linear least square estimation for the six-parameter gyroscope calibration model.

The contribution of this paper can be summarized as follows. First, a efficient servomotor-aided gyroscope calibration method is proposed. It is worth to note that no high precision equipment is used during the calibration. Secondly, a six-point G-optimal experiment is proposed for the gyroscope calibration. The proposed DoE can significantly shorten the calibration time and has been experimentally tested. Thirdly, a fast converged recursive linear least square estimation method

L. Wang and S. W. Su are with Faculty of Engineering and IT, University of Technology Sydney, Sydney, NSW 2007, Australia (e-mail: steven.su@uts.edu.au).

This work has been submitted to the IEEE for possible publication. Copyright may be transferred without notice, after which this version may no longer be accessible.

is proposed to reduce the computational complexity, which allows the calibration work is more suitable for an embedded environment.

This paper is organized as follows. In section II, the proposed calibration method and the DoE is discussed. In Section III, we validate the proposed method using simulation under different conditions. Section IV demonstrates the implementation of the proposed method on two commonly used gyroscopes. Section V concludes this paper.

II. CALIBRATION METHODOLOGY

A. Efficient Calibration Method for Triaxial Gyroscope

Various factors contribute to the error in a gyroscope. In this study, scale factors and biases are considered as error sources. Thus, a 6-parameter calibration model is employed to define the unknown parameters. The relation between the true angular velocity $\mathbf{G}_i = [g_{x,i}, g_{y,i}, g_{z,i}]^T$ and the measured angular velocity $\mathbf{M}_i = [m_{x,i}, m_{y,i}, m_{z,i}]^T$ at i th observation are described as:

$$\begin{bmatrix} g_{x,i} \\ g_{y,i} \\ g_{z,i} \end{bmatrix} = \begin{bmatrix} k_x & 0 & 0 \\ 0 & k_y & 0 \\ 0 & 0 & k_z \end{bmatrix} \left(\begin{bmatrix} m_{x,i} \\ m_{y,i} \\ m_{z,i} \end{bmatrix} + \begin{bmatrix} b_x \\ b_y \\ b_z \end{bmatrix} \right) \quad (1)$$

where k_x, k_y, k_z and b_x, b_y, b_z stand for the scale factor and the bias of each axis, respectively.

The idea of this method is that the measurement of gyroscope should be equal to the rotation speed, that is

$$\omega_i = \sqrt{g_{x,i}^2 + g_{y,i}^2 + g_{z,i}^2} \quad (2)$$

where ω_i is the rotation speed.

We can expend Eq.(2) and square both side of the equation. Then, we have:

$$\begin{aligned} \omega_i^2 &= k_x^2 m_{x,i}^2 + k_y^2 m_{y,i}^2 + k_z^2 m_{z,i}^2 \\ &+ 2k_x^2 b_x m_{x,i} + 2k_y^2 b_y m_{y,i} + 2k_z^2 b_z m_{z,i} \\ &+ \sum_{j=x,y,z} k_j^2 b_j^2 + \epsilon_i \end{aligned} \quad (3)$$

The error term ϵ_i is a combination of a Gaussian and a noncentral Chi-squared noise. Similar to [18], the Chi-squared noise term can be ignored when the rotating speed is high. Thus, in this study, we consider the ϵ_i as a Gaussian noise. If we let

$$\begin{cases} \beta_0 = \sum_{j=x,y,z} k_j^2 b_j^2 \\ \beta_1 = k_x^2 \\ \beta_2 = k_y^2 \\ \beta_3 = k_z^2 \\ \beta_4 = 2k_x^2 b_x \\ \beta_5 = 2k_y^2 b_y \\ \beta_6 = 2k_z^2 b_z \end{cases} \quad \begin{cases} x_{1,i} = m_{x,i}^2 \\ x_{2,i} = m_{y,i}^2 \\ x_{3,i} = m_{z,i}^2 \\ x_{4,i} = m_{x,i} \\ x_{5,i} = m_{y,i} \\ x_{6,i} = m_{z,i} \end{cases} \quad y_i = \omega_i^2,$$

then the gyroscope calibration problem becomes

$$y_i = \beta_0 + \beta_1 x_{1,i} + \beta_2 x_{2,i} + \beta_3 x_{3,i} + \beta_4 x_{4,i} + \beta_5 x_{5,i} + \beta_6 x_{6,i} + \epsilon_i, \quad (4)$$

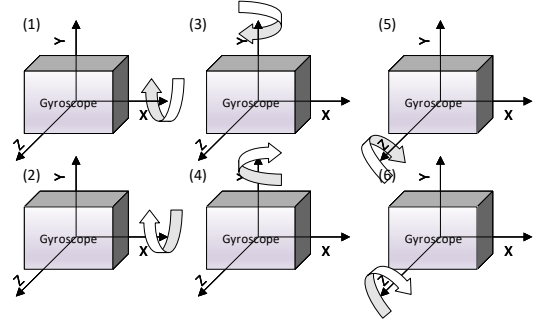


Fig. 1. 6-observations rotation protocol for gyroscope calibration. Rotate the gyroscope at constant speed clockwise and counterclockwise along the x,y,z axis.

which is a linear regression problem. The cost function of this problem is defined as:

$$J = \sum_{i=1}^n (||y_i - y_{true,i}||) \quad (5)$$

where y_{true} is the squared rotation speed provided by the servomotor. However, there is no close form solutions for this problem as the parameter β_0 can be represented by the remaining six parameters $\beta_0 = \frac{\beta_4^2}{4\beta_1} + \frac{\beta_5^2}{4\beta_2} + \frac{\beta_6^2}{4\beta_3}$. The representation introduces the nonlinearity to the Eq.(4). Thus, the problem can be solved using the nonlinear regression technic such as Levenberg-Marquardt algorithm [17]. In practice, a gyroscope is often a part of an embedded system with limited resource and battery life. To reduce the computational complexity, a novel iterative least square method [13] is employed to estimate the parameters.

We can reform Eq.(4) in matrix form as:

$$Y = X\beta + \beta_0 + \epsilon \quad (6)$$

The observation matrix $X \in \mathbb{R}^{6 \times 6}$ consists of the measured angular velocity:

$$X = \begin{bmatrix} m_{x,1} & m_{y,1} & m_{z,1} & m_{x,1}^2 & m_{y,1}^2 & m_{z,1}^2 \\ m_{x,2} & m_{y,2} & m_{z,2} & m_{x,2}^2 & m_{y,2}^2 & m_{z,2}^2 \\ m_{x,3} & m_{y,3} & m_{z,3} & m_{x,3}^2 & m_{y,3}^2 & m_{z,3}^2 \\ m_{x,4} & m_{y,4} & m_{z,4} & m_{x,4}^2 & m_{y,4}^2 & m_{z,4}^2 \\ m_{x,5} & m_{y,5} & m_{z,5} & m_{x,5}^2 & m_{y,5}^2 & m_{z,5}^2 \\ m_{x,6} & m_{y,6} & m_{z,6} & m_{x,6}^2 & m_{y,6}^2 & m_{z,6}^2 \end{bmatrix} \quad (7)$$

The response matrix $Y = [y_{true,1}, y_{true,2}, \dots, y_{true,6}]^T$, parameters $\beta = [\beta_1, \beta_2, \dots, \beta_6]^T$, bias term $\beta_0 \in \mathbb{R}^{1 \times 6} = [\beta_0, \beta_0, \dots, \beta_0]^T$, and noise term $\epsilon = [\epsilon_1, \epsilon_2, \dots, \epsilon_6]^T$.

For solving Eq.(6), the fast converged iterative least square method is summarized in Algorithm 1. The convergent condition is given as $0 \leq \beta_0 < 0.5$ [13]. For a low cost MEMS gyroscope, the scale factor is usually between 0.8 and 1.2. The bias term is usually between $\pm 0.1 \text{ rad/s}$. Recall that $\beta_0 = \sum_{j=x,y,z} k_j^2 b_j^2$. Obviously, the convergence condition is met.

B. G-Optimal Experimental Design

Unlike an accelerometer, it is hard for a low-cost MEMS gyroscope to do autocalibration using the Earth's rotation.

Algorithm 1: Iterative least square method

Result: Estimated scale factors $[k_x, k_y, k_z]$ and bias $[b_x, b_y, b_z]$

Set initial value $\beta_0^{(0)} = [0, 0, 0, 0, 0, 0]$;

Calculate initial estimation

$$\beta^{(1)} = (X^T X)^{-1} X^T (Y - \beta_0^{(0)});$$

while $\sum_{j=1}^6 \|\beta_j^{(n+1)} - \beta_j^{(n)}\| > 10^{-6}$ **do**

Update β_0 at n th iteration as follows:

$$\beta_0^{(n)} = \frac{\beta_4^{2(n)}}{4\beta_1^{(n)}} + \frac{\beta_5^{2(n)}}{4\beta_2^{(n)}} + \frac{\beta_6^{2(n)}}{4\beta_3^{(n)}};$$

$$\beta_0^{(n)} = [\beta_0^{(n)}, \beta_0^{(n)}, \beta_0^{(n)}, \beta_0^{(n)}, \beta_0^{(n)}, \beta_0^{(n)}];$$

Update β at n th iteration as follows:

$$\beta^{(n+1)} = (X^T X)^{-1} X^T (Y - \beta_0^{(n)})$$

end

return Scale factors and bias terms:

$$\begin{cases} k_x = \sqrt{\beta_1} \\ k_y = \sqrt{\beta_2} \\ k_z = \sqrt{\beta_3} \end{cases} \begin{cases} b_x = \frac{\beta_4}{2\beta_1} \\ b_y = \frac{\beta_5}{2\beta_2} \\ b_z = \frac{\beta_6}{2\beta_3} \end{cases}$$

The Earth rotates at a moderate angular velocity of $7.29 \times 10^{-5} \text{ rad/s}$, which is far less than the bias term of the gyroscope. Thus, an external device, servomotor, is employed in this study. Considering the working principle of a servomotor, it may have vibrations during operation, but the time per revolution can be very accurate. Owing to the linearity of Eq.(4), we can take the average of both sides of the equation during each revolution and consider it as one observation. In this case, we can minimize the influences of vibrations and random noise to the estimated parameter.

The linear regression problem includes the estimation of six parameters. Thus, at least six observations are required [19]. To minimizing the maximum variance of the estimated parameters, we introduce a G-optimal design of a second order three variables model Eq. (4) for gyroscope calibration experiments. As the measurement is limited by $m_{x,i}^2 + m_{y,i}^2 + m_{z,i}^2 \approx \omega_i^2$, the design region is spherical. For a 6-observations experimental scheme, the G-optimal design matrix can be expressed as:

$$D = \begin{matrix} & m_{x,i} & m_{y,i} & m_{z,i} \\ \begin{pmatrix} 1 \\ 2 \\ 3 \\ 4 \\ 5 \\ 6 \end{pmatrix} & \begin{bmatrix} 1 & 0 & 0 \\ -1 & 0 & 0 \\ 0 & 1 & 0 \\ 0 & -1 & 0 \\ 0 & 0 & 1 \\ 0 & 0 & -1 \end{bmatrix} \end{matrix}$$

Accordingly, the rotation method of the gyroscope is shown in Fig.1. We rotate the gyroscope 360 degrees clockwise and counterclockwise along the x,y,z axis at the speed of ω , respectively. We average the data during each rotation and construct the 6-by-6 observation matrix according to Eq.(7). It is worth noting that no high-precise device is used to eliminate the alignment error. Once this 6-observation matrix is constructed, the scale factors and bias terms can be calculated using Algorithm 1.

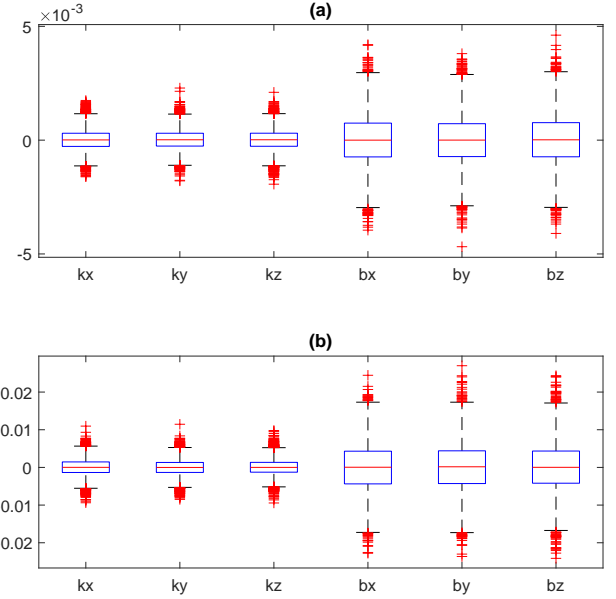


Fig. 2. The simulation results of estimation error between estimated parameters and true parameters under normal conditions at different noise level. (a)0.035 rad/s noise level. (b)0.2 rad/s noise level

III. SIMULATION

With the intention of validating the feasibility of the proposed calibration method under the different weight of scale factors, biases, rotation speed, orientation misalignment, and noise level, we first examine the proposed method using simulations. During each simulation, we generate a set of parameters under certain condition, and these parameters are considered as the ground truth. Based on the true value, measurements of six observations are generated according to the experiment protocol in Fig.1. Then, the proposed method was employed to calculate the scales and biases based on the generated measurements, and the estimated parameters were stored.

A. Simulation Under Normal Conditions

We first test the calibration method similar to the hardware constraints. The following assumptions on the parameter are given, and the results are explained after them.

- 1) The scale factor follows a uniform distribution $U(80\%, 120\%)$ and the bias follows $U(-0.1 \text{ rad/s}, 0.1 \text{ rad/s})$. The typical scale factors and biases of low-cost MEMS gyroscopes are usually within $\pm 20\%$ and $\pm 0.1 \text{ rad/s}$, respectively.
- 2) Misalignment on mounting follows $U(0\%, 10\%)$. In practice, without accurate mounting platform, it is hard for users to make measurements in the exact position of the experiment protocol. To show the robustness of the proposed method, we show the simulations with mounting misalignment.
- 3) The measurement noise is assumed following Gaussian distribution with zero mean and two different variance, which are $\epsilon_1 \sim \mathcal{N}(0, 0.035)$ and $\epsilon_2 \sim \mathcal{N}(0, 0.2)$. The typical noise spectral density of the MEMS gyroscope

is between $0.01 \sim 0.05 \text{ deg/s}/\sqrt{Hz}$. As a 200 Hz sampling rate is used in this study, the range of noise amplitude is around $0.035 \sim 0.18 \text{ rad/s}$. Thus, we consider the noise vibration as 0.035 and 0.2 rad/s .

- 4) The variance of rotation noise is five percents of the current speed, which follows $\mathcal{N}(0, 5\%\omega)$. We use this term to simulate the vibration during operation.

Based on the assumptions, we generated the 30 different sets of scale factors and biases to simulate different gyroscopes. For each set of parameters, 500 times simulations were repeated. For each simulation, we take a 6-observation measurement according to the experiment protocol shown in Fig.1 and we construct a 6-by-6 observation matrix based on Eq.(7). Subsequently, Algorithm 1 was implemented to estimate the scale factors and the biases. Overall, 15000 simulations were generated for testing the proposed calibration method.

To evaluate the performance of the proposed calibration method, we calculated the differences between the true parameters and the estimated scale factors and biases. Box plots were used to analysis the differences as shown in Fig.2. The median values of the estimation error are 0, and the results indicate the estimated parameters are unbiased. The majority of estimations have an error within $\pm 8 \times 10^{-4}$ for the 0.035 rad/s noise level and $\pm 4.5 \times 10^{-3}$ for 0.2 rad/s noise level. This indicates that the estimation accuracy is also related to the measurement noise level. Better gyroscopes with lower noise get lower estimation error. Interestingly, the scale factors have a much lower estimation error than the biases terms do. This phenomenon can be explained by sensitivity analysis techniques [20]. In this particular model Eq.(4) and experiment design, the observability of scale factors is much higher than that of bias terms, which lead to better estimation results for scale factors. Besides, for the purpose of intuitively demonstrating the effectiveness of the calibration, we run a simulation to compare the gyroscope readings before and after calibration. The desired rotation speed of the servomotor ω respect to time was set to be a sine wave with an amplitude of 1 rad/s and frequency of $\frac{3}{4} \text{ Hz}$. The three axes of the gyroscope are mounted to be equidistant from thee rotation axis. Thus, the projection of the rotation speed to each axis is equal. The variance of rotation noise is set to be 5% of the current speed, and the measurement noise follows $\epsilon \sim \mathcal{N}(0, 0.035)$. We randomly generation a set of parameter and use the proposed method to estimate the scale factors and bias terms. The true parameters $[k_x, k_y, k_z, b_x, b_y, b_z]$ and estimated parameters $[\hat{k}_x, \hat{k}_y, \hat{k}_z, \hat{b}_x, \hat{b}_y, \hat{b}_z]$ are as follow:

$$\begin{cases} k_x = 0.9070 \\ k_y = 1.0501 \\ k_z = 0.8734 \\ b_x = 0.0528 \\ b_y = 0.0813 \\ b_z = -0.0992 \end{cases} \quad \begin{cases} \hat{k}_x = 0.9070 \\ \hat{k}_y = 1.0502 \\ \hat{k}_z = 0.8735 \\ \hat{b}_x = 0.0529 \\ \hat{b}_y = 0.0802 \\ \hat{b}_z = -0.0994 \end{cases}$$

Based on the estimated parameters, we corrected the gyroscope readings using Eq.(1). Fig.3 demonstrates that after calibration, the fitness between the measured value and the true

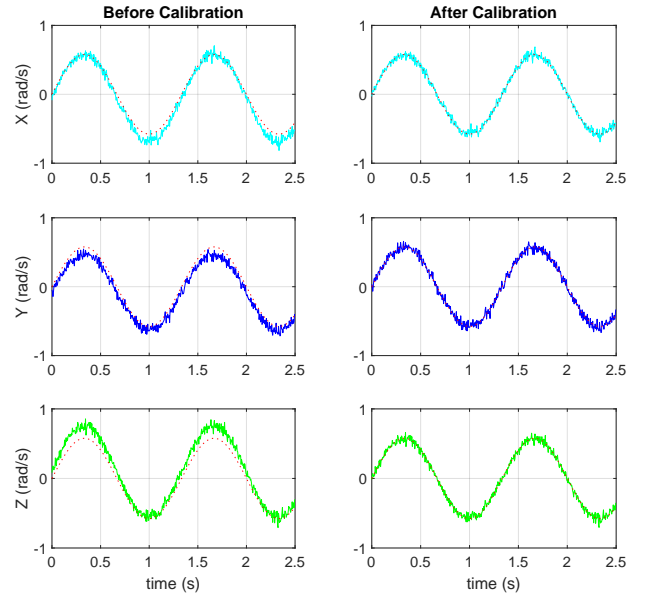


Fig. 3. The simulation results of the desired rotation speed ω and gyroscope readings from three axes x, y, z before and after calibration. Dashed line indicates true rotation on each axis and solid line represents gyroscope readings

value is higher. The fluctuations were caused by measurement noise and motor speed instability.

B. The Effect of the Rotation Speed

Next, we explore the influence of the rotation speed on the estimation results during calibration. We followed the 15000 simulations procedure mentioned above except for using different rotation speed. The rotation speed is set to be from 0.3 to 3 rad/s with a step size of 0.1 rad/s . Insufficient rotation speed may be covered by noise while rapid rotations cannot be achieved by servomotors accurately during real experiment. The overall mean squared error (MSE) of six estimated parameters are defined as follow:

$$e_j = \frac{1}{N} \sum_{i=1}^N (j_i - \hat{j}_i)^2, j_i = k_{x,i}, k_{y,i}, k_{z,i}, b_{x,i}, b_{y,i}, b_{z,i} \quad (8)$$

where N is the number of simulations. Fig.4 shows the influence of speed on the parameter estimation accuracy during calibration. As the speed increases, the average MSE decreases exponentially. After the speed rises to 1 rad/s , the average MSE value basically does not decrease. Regardless of the speed changes, the MSE of biases remains unchanged. It is only affected by the measurement noise level. Because even in a static state, i.e. $\omega = 0$, the observability of biases still exists. Appealingly, when the speed is less than 1 rad/s , as the speed increases, the MSE of scales factors drops significantly. At low speeds, the measurement noise occupies most of the measured value rather than the projection of the rotation component on this axis. At this time, the signal to noise ratio (SNR) of the measured value is small. The lower the rotation speed, the smaller the SNR. At the same rotation speed, when comparing the (a) and (b) in Fig.4, the estimation with high measurement noise has a larger MSE.

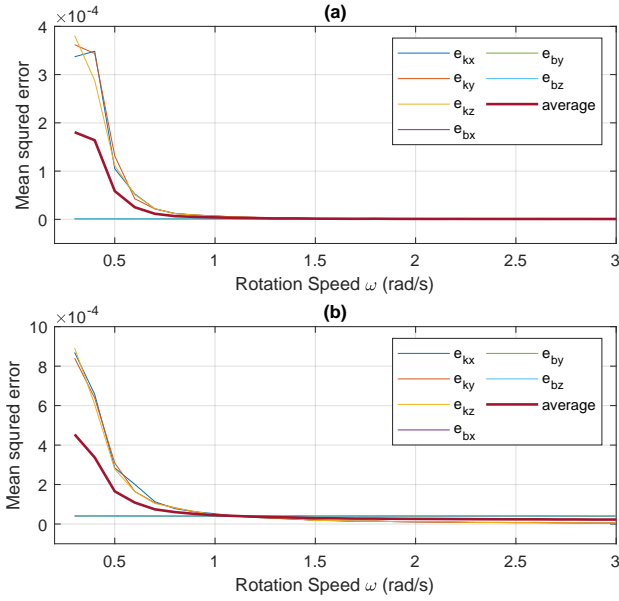


Fig. 4. The MSE between estimated parameters and true parameters at different rotation speed during calibration period with different measurement noise (a)0.035 rad/s noise level. (b)0.2 rad/s noise level

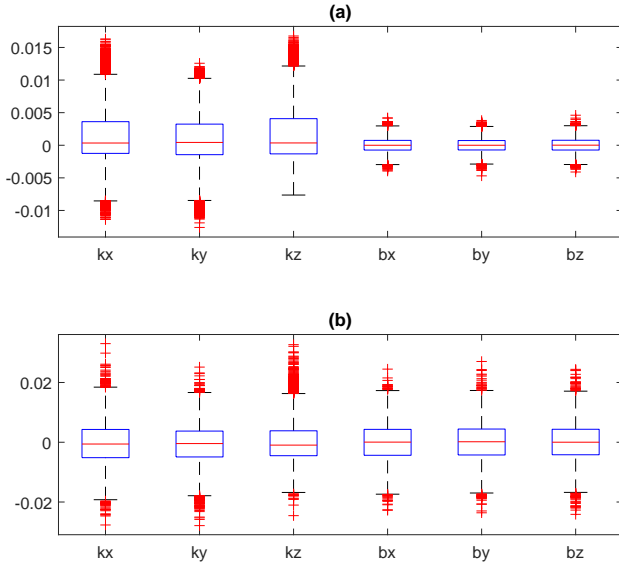


Fig. 5. The simulation results of estimation error between estimated parameters and true parameters under extreme conditions at different noise level. (a)0.035 rad/s noise level. (b)0.2 rad/s noise level

C. The Robustness under Extreme Conditions

To show the robustness of the proposed gyroscope calibration method, the quality of the gyroscope was assumed to be very poor. The random generated parameters follows $U(120\%, 200\%)$ for scale factors and $U(-0.2 \sim -0.1, 0.1 \sim 0.2)$ for biases. Other parameters follow the previous setting. The results shown in Fig.5 points out that the method presented in this paper is applicable to the gyroscopes with poor manufacture quality. Although the errors are larger than normal conditions, the majority of error are within $\pm 4 \times 10^{-3}$ for 0.035 rad/s noise level and $\pm 4.5 \times 10^{-3}$ for 0.2 rad/s noise

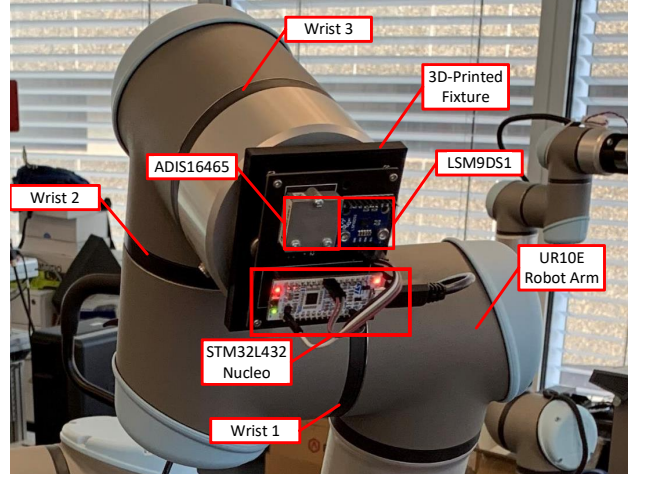


Fig. 6. Experimental system for the gyroscope calibration on a robot arm UR10e. The part names and joint numbers are noted.

level. This time, the scale factors have worse observability as the larger scale factors enlarge the signal noise. Thus, the SNR is reduced.

To demonstrate the convergence rate of the iterative method, we run the three simulations, and the results are shown in TABLE I. The first simulation consists of high scale factors error and normal biases, while the second simulation contains normal scale factors error and high biases. Simulation 3 uses high scales factors error and high biases. The results show that less than three iterations are needed for the proposed calibration method.

TABLE I
CONVERGENCE RATE UNDER DIFFERENT SCALE FACTORS AND BIASES

Number of iterations	k_x	k_y	k_z	b_x	b_y	b_z
1.High scale factor error						
True value	1.9074	1.9529	1.5635	0.0827	0.0265	-0.0805
1	1.9102	1.9571	1.5665	0.0822	0.0243	-0.0797
2-Converged	1.9071	1.9539	1.5640	0.0822	0.0243	-0.0797
2.High bias						
True value	1.0979	1.1052	0.9851	-0.1046	0.1995	0.1565
1	1.1029	1.1103	0.9900	-0.1057	0.1971	0.1545
2	1.0961	1.1035	0.9839	-0.1057	0.1971	0.1545
3-Converged	1.0962	1.1036	0.9840	-0.1057	0.1971	0.1545
3.High scale factor error and bias						
True value	1.5044	1.6494	1.5282	0.1483	-0.1282	0.1794
1	1.5173	1.6652	1.5423	0.1469	-0.1284	0.1802
2	1.5053	1.6521	1.5302	0.1469	-0.1285	0.1803
3-Converged	1.5055	1.6523	1.5304	0.1469	-0.1285	0.1803

IV. EXPERIMENT

We calibrated and verified two commonly used low-cost MEMS gyroscopes which are LSM9DS1 from STMicroelectronics and MPU9250 from TDK. We demonstrated the proposed method on a UR10e robotic arm. We also 3D-printed a fixture to mount the gyroscopes onto the arm. The calibration system is shown in Fig.6. The gyroscope is replaceable. The digital signals are collected and calculated using an STM32L432 Nucleo board. It is worth noting that high-precision turntables or other calibration equipment are

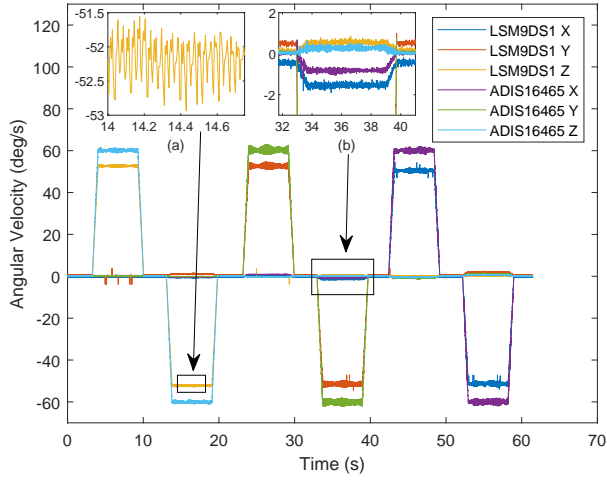


Fig. 7. Raw gyroscope data from LSM9DS1 comparing with ADIS16465 reading during calibration period. (a) The periodic vibration is caused by the control strategy of the servomotor. (b) The component on non-rotating axis is caused by mounting misalignment.

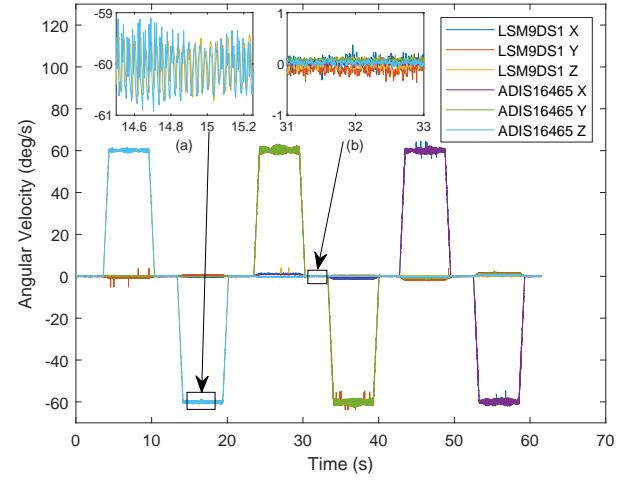


Fig. 9. Calibrated gyroscope data from LSM9DS1 comparing with ADIS16465 reading during testing period. (a) The reading from LSM9DS1 and ADIS16465 nearly coincide with each other. (b) The biases of gyroscope reading are almost zero.

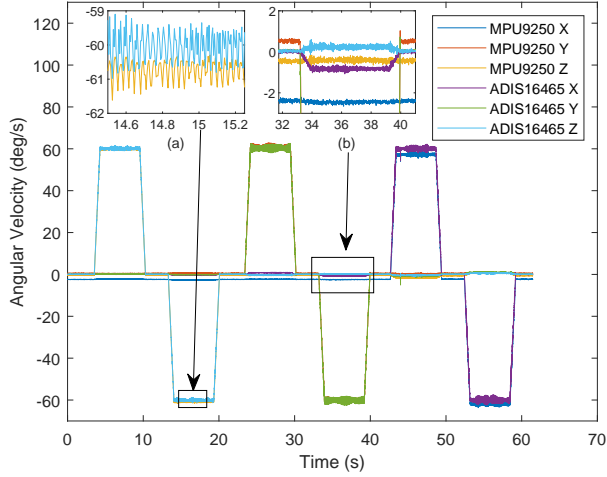


Fig. 8. Raw gyroscope data from MPU9250 comparing with ADIS16465 reading during calibration period. (a) The periodic vibration is caused by the control strategy of the servomotor. (b) The component on non-rotating axis is caused by mounting misalignment.

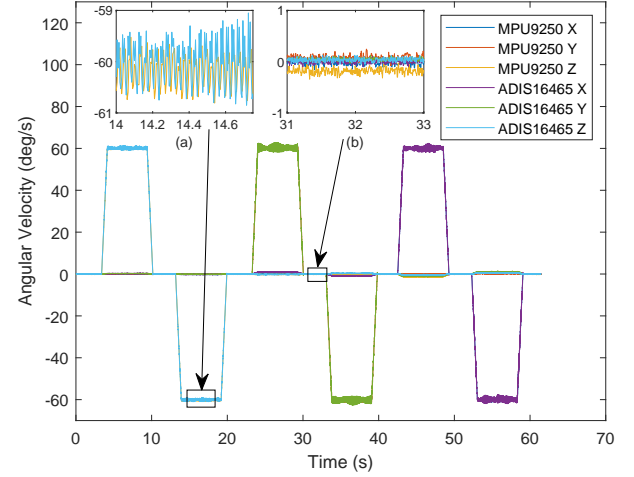


Fig. 10. Calibrated gyroscope data from MPU9250 comparing with ADIS16465 reading during testing period. (a) The reading from MPU9250 and ADIS16465 nearly coincide with each other. (b) The biases of gyroscope reading are almost zero.

not used in the proposed system. For the purpose of comparing the data quality of low-cost gyroscopes, an ADIS16465 sensor was mounted on the same board during calibration. The ADIS16465 was pre-calibrated using a turntable. The room temperature was set to 22 °C.

A. Calibration of Two Low-cost Gyroscopes

The proposed method was applied to the gyroscopes according to the G-optimal experiment scheme shown in Fig.1. We can summarise the calibration procedure as follows:

- 1) Mount the LSM9DS1 and ADIS16465 on the UR10e and turn on the system.
- 2) Rotate the wrist 3 of the UR10e for 360° clockwise. Based on the simulation results, to find the balance between the rotation speed and the measurement noise,

the angular velocity is set to 60°/s. Then, Wait for 3 seconds.

- 3) Rotate the wrist 3 of the UR10e for 360° counterclockwise. Wait for 3 seconds.
- 4) Repeat 2-3 for wrist 1 and wrist 2.
- 5) Repeat 1-4 for MPU9250.

The entire process lasts about one minute. The data was recorded by the microcontroller and transferred to the computer via a serial port. After the calibration process finished on the microcontroller, the scale factors and biases transfer to the computer as well. The raw data from LSM9DS1 and MPU9250 are shown in Fig.7 and Fig.8. From the figure, we can see that the readings of the two sensors are quite different from the readings from ADIS16465. As the ADIS16465 is a high-precision sensor and we have pre-calibrated it, we can infer that the difference is caused by the scale factors and

biases of the low-cost sensors. The servomotor control strategy leads to the vibration during rotation, while the ADIS16465 reading infers that the average angular velocity is relatively accurate. Due to high-precision components are not used in the mounting process, the non-rotating axis also has some rotation component. This can prove that the proposed method can work under conditions of vibration and misalignment.

To demonstrate the accuracy of the proposed method, we compared the calibration results with the precision turntable methods [7]. The results are shown in TABLE II and TABLE III. For a fast calibration method without any high-precise

TABLE II
CALIBRATION RESULTS COMPARISON OF LSM9DS1

Parameter	Results of proposed calibration method	Results of conventional turntable method
k_x	1.1775	1.1771
k_y	1.1552	1.1554
k_z	1.1445	1.1440
$b_x(rad/s)$	0.0076	0.0077
$b_y(rad/s)$	-0.0103	-0.0100
$b_z(rad/s)$	-0.0042	-0.0051

TABLE III
CALIBRATION RESULTS COMPARISON OF MPU9250

Parameter	Results of proposed calibration method	Results of conventional turntable method
k_x	1.0069	1.0065
k_y	0.9960	0.9955
k_z	0.9955	0.9950
$b_x(rad/s)$	0.0442	0.0411
$b_y(rad/s)$	-0.0089	-0.0099
$b_z(rad/s)$	0.0076	0.0101

equipment, all errors less than 10^{-3} is a considerable accurate result. Besides, considering the low-repeatability of these two gyroscopes, the true scale factors and biases when on the robot arm maybe different from those when on the turntable.

After calibration, the parameters are stored in the microcontroller. To further test the effect of calibration, the robot

arm repeats the same movements as during the calibration procedure. Instead of raw data, the microcontroller sends the calibrated gyroscope reading to the computer. The results after calibration are shown in Fig.9 and Fig.10. The reading from pre-calibrated ADIS16465 is considered as a ground truth. We calculated the mean square error (MSE) error between the LSM9DS1/MPU9250 and ADIS16465. The details are shown in TABLE IV and TABLE V. Experiments show that the gyroscope reading obtained after calibration using the proposed method is significantly more accurate than the reading before calibration.

V. CONCLUSION

This paper proposed an efficient servomotor-aided calibration method that estimates the gain factors and biases of a triaxial gyroscope. A 6-observation G-optimal experimental scheme was proposed for the calibration process. Besides, a fast converged recursive linear least square estimation method was proposed to reduce the computational complexity. To verify the validity of the presented method, simulations and experiments have been done.

The simulation results indicated that the gyroscope parameter could be estimated accurately within three iterations and demonstrated that the method is robust under extreme condition. Besides, the simulation results found the balance between the rotation speed and the measurement noise. The angular velocity in the experiment was set to $60^\circ/s$, accordingly.

The experiments were performed on two commonly used low-cost MEMS gyroscope. The outcome of the proposed method and the conventional turntable method were compared in the experiment. The results indicate that the errors between these two methods were less than 10^{-3} . To further test the effect of the proposed method, we compared the calibrated reading of these two low-cost with a high-precision sensor. The outcome showed that the error significantly decreased after calibration. More importantly, we demonstrate the implementation possibility of this method on low-precision motors such as a robot arm and the achievability of the proposed method on a microprocessor. It is worth to note that the entire calibration only took one minute and high-precision calibration equipment was not used.

TABLE IV
MSE BETWEEN LSM9DS1 AND ADIS16465

Axis	Error before calibration (rad/s)	Error after calibration (rad/s)
x	0.2798	0.0052
y	0.2255	0.0093
z	0.1940	0.0022

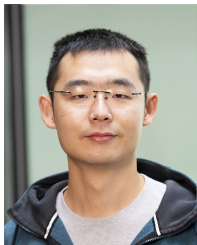
TABLE V
MSE BETWEEN MPU9250 AND ADIS16465

Axis	Error before calibration (rad/s)	Error after calibration (rad/s)
x	0.1031	0.0051
y	0.0107	0.0057
z	0.0096	0.0033

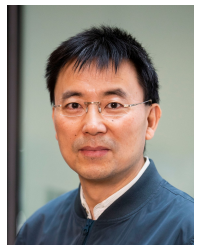
REFERENCES

- [1] M. Ma, Q. Song, Y. Gu, and Z. Zhou, "Use of magnetic field for mitigating gyroscope errors for indoor pedestrian positioning," *Sensors*, vol. 18, no. 8, p. 2592, 2018.
- [2] M. Khedr and N. El-Sheimy, "A smartphone step counter using imu and magnetometer for navigation and health monitoring applications," *Sensors*, vol. 17, no. 11, p. 2573, 2017.
- [3] K. Han, H. Han, Z. Wang, and F. Xu, "Extended kalman filter-based gyroscope-aided magnetometer calibration for consumer electronic devices," *IEEE Sensors Journal*, vol. 17, no. 1, pp. 63–71, 2016.
- [4] M. B. Rhudy and J. M. Mahoney, "A comprehensive comparison of simple step counting techniques using wrist-and ankle-mounted accelerometer and gyroscope signals," *Journal of Medical Engineering & Technology*, vol. 42, no. 3, pp. 236–243, 2018.
- [5] P. Zhang, X. Zhan, X. Zhang, and L. Zheng, "Error characteristics analysis and calibration testing for mems imu gyroscope," *Aerospace Systems*, vol. 2, no. 2, pp. 97–104, 2019.
- [6] H. Yang, B. Zhou, L. Wang, H. Xing, and R. Zhang, "A novel tri-axial mems gyroscope calibration method over a full temperature range," *Sensors*, vol. 18, no. 9, p. 3004, 2018.

- [7] A. B. Chatfield, *Fundamentals of high accuracy inertial navigation*. American Institute of Aeronautics and Astronautics, 1997.
- [8] M. Hwangbo, J.-S. Kim, and T. Kanade, "Imu self-calibration using factorization," *IEEE Transactions on Robotics*, vol. 29, no. 2, pp. 493–507, 2013.
- [9] Y. Wu and L. Pei, "Gyroscope calibration via magnetometer," *IEEE Sensors Journal*, vol. 17, no. 16, pp. 5269–5275, 2017.
- [10] A. Olivares, G. Olivares, J. Gorriz, and J. Ramirez, "High-efficiency low-cost accelerometer-aided gyroscope calibration," in *2009 International Conference on Test and Measurement*, vol. 1. IEEE, 2009, pp. 354–360.
- [11] C. Ren, Q. Liu, and T. Fu, "A novel self-calibration method for mimu," *IEEE Sensors Journal*, vol. 15, no. 10, pp. 5416–5422, 2015.
- [12] S.-h. P. Won and F. Golnaraghi, "A triaxial accelerometer calibration method using a mathematical model," *IEEE transactions on instrumentation and measurement*, vol. 59, no. 8, pp. 2144–2153, 2009.
- [13] L. Ye, Y. Guo, and S. W. Su, "An efficient autocalibration method for triaxial accelerometer," *IEEE Transactions on Instrumentation and Measurement*, vol. 66, no. 9, pp. 2380–2390, 2017.
- [14] S.-h. P. Won and F. Golnaraghi, "A triaxial accelerometer calibration method using a mathematical model," *IEEE transactions on instrumentation and measurement*, vol. 59, no. 8, pp. 2144–2153, 2009.
- [15] U. Qureshi and F. Golnaraghi, "An algorithm for the in-field calibration of a mems imu," *IEEE Sensors Journal*, vol. 17, no. 22, pp. 7479–7486, 2017.
- [16] J. A. Nelder and R. Mead, "A simplex method for function minimization," *The computer journal*, vol. 7, no. 4, pp. 308–313, 1965.
- [17] G. A. Seber and C. J. Wild, "Nonlinear regression. hoboken," *New Jersey: John Wiley & Sons*, vol. 62, p. 63, 2003.
- [18] I. Frosio, F. Pedersini, and N. A. Borghese, "Autocalibration of triaxial mems accelerometers with automatic sensor model selection," *IEEE Sensors Journal*, vol. 12, no. 6, pp. 2100–2108, 2012.
- [19] J. Kiefer and J. Wolfowitz, "The equivalence of two extremum problems," *Canadian Journal of Mathematics*, vol. 12, pp. 363–366, 1960.
- [20] J. C. Helton, "Uncertainty and sensitivity analysis techniques for use in performance assessment for radioactive waste disposal," *Reliability Engineering & System Safety*, vol. 42, no. 2-3, pp. 327–367, 1993.



Li Wang received the Bachelor of Engineering degree from the Wuhan University in 2016 and Master of Engineering degree from the Australia National University in 2019. He is currently a PhD student at Faculty of Engineering and Information Technology, UTS, and perusing his research career in Biomedical Engineering. Li's research interests are on embedded system design, wearable health monitoring system design, IMU calibration, cardiovascular rehabilitation system design and reinforcement learning control.



Steven W. Su (M'99-SM'17) received the B.S. and M.S. degrees from the Harbin Institute of Technology, Harbin, China, in 1990 and 1993, respectively, and the Ph.D. degree from the Research School of Information Sciences and Engineering, Australian National University, Canberra, Australia, in 2002.

He was a Post-Doctoral Research Fellow with the Faculty of Engineering, University of New South Wales, Sydney, NSW, Australia, from 2002 to 2006. He is currently an Associate Professor with the Faculty of Engineering and Information Technology, University of Technology Sydney, Sydney, Australia. His current research interests include biomedical system modeling and control, nonlinear robust control, fault tolerant control, and wearable monitoring systems.